

Holistic Approach to the System Optimization of a Proportional Valve

Artemi Makarow*, Jan Braun*, Martin Keller**, Torsten Bertram*, Georg Schoppel***, Ingo Glowatzky***

TU Dortmund University, Institute of Control Theory and Systems Engineering, Otto-Hahn-Str. 8, D-44227 Dortmund, Germany* (Former Institute Member**)
Bosch Rexroth AG, Partensteiner Str. 23, D-97816 Lohr am Main, Germany***
E-Mail: artemi.makarow@tu-dortmund.de

This contribution presents a holistic approach to the system optimization of a highly dynamic proportional valve. The model with lumped parameters which is used for the evaluation of the closed-loop performance is parameterized based on Finite-Element-Method (FEM) data. In addition to the calculation of static characteristic curves, a suitable excitation signal is applied to the transient FEM simulation. The valve dynamics of the current geometrical valve design are identified using the transient simulation results. This new approach enables a fully automated system optimization of a proportional valve. Hence, during the optimization, human expertise is not required.

Keywords: System Optimization, System Identification, Holistic Model, Highly Dynamic Proportional Valve
Target audience: Design Process, Components, Industrial Applications

1 Introduction

A proportional directional control valve represents a mechatronic system. Different domains like electrical engineering, mechanics, and hydraulics are merged into a single mechatronic system. The result is a nonlinear system with fast dynamics which is difficult to control. An insight into the development process of mechatronic systems illustrates the sequential and mostly independent development of the individual subsystems. During this development, objectives are used which refer to the characteristics of the respective subsystem as maximizing force and torque, minimizing friction and movable mass. In the case of hydraulic valves, these subsystems are designed to reach the desired hydraulic characteristics of the whole system theoretically with consideration of safety aspects. Domain-specific modeling and simulation tools are utilized and are supported by human expertise. After a certain level of development is reached, the subsystems are assembled into a mechatronic system. From that moment, the overall system performance is essential. To evaluate the system performance a suitable control concept and power electronics are needed. Hence, the closed-loop performance highlights the system quality and proves whether the characteristics of the different subsystems fit each other. However, the characteristics of the several hardware subsystems which are suited best for closed-loop operations are not known precisely in advance. The controller is designed to reach the required system performance and to overcome the possible shortcomings of the hardware subsystems. The problem of the sequential development is for instance discussed in /1/ and /2/. Due to the strong nonlinearities of some mechatronic systems, an advanced control concept is required. Regarding industrial applications, cascaded control concept based on nonlinear PID controller are widespread. The reasons for this are the well-studied PID theory and their low computational effort /3/. To reach pre-defined system performance requirements regarding the whole operating range, the controllers are extended with nonlinear characteristic curves for the integral and proportional amplification. Hence, the controller parameters depend on the control error $e(t)$. The high number of coupled controller parameters requires a fully automated Hardware-in-the-Loop (HiL) optimization. In /4/ a multi-criteria evolutionary optimization process for hydraulic valve controllers is presented and is suitable for at least 24 controller parameters. Although this optimization is time expensive, it is the only possibility to adjust the system performance after the mechatronic system hardware is

build. Obviously, there is a need to develop a holistic system optimization procedure including optimization of design parameters like geometrical parameters as well as controller parameters. To optimize the hardware design time- and cost-efficiently a model-based approach must be used. The challenge is to develop a holistic simulation environment which can connect the different domains of a mechatronic system and enable controller optimization with an acceptable time effort. Usually, each subsystem is related to a domain-specific modelling tool and a numerical simulation method. Regarding the holistic model-based system optimization, two objectives contrast with each other. To improve the hardware design of a mechatronic system a model with a high level of detail including geometrical parameters is required. The clear impacts of design parameter variations on the physical interactions within a subsystem are essential. Numerical simulation methods to solve approximately partial differential equations like the Finite-Element-Method (FEM) or the Computational Fluid Dynamics (CFD) are well suited for this task. However, they come along with a high computational effort. On the other hand evaluating the closed-loop performance is of particular interest. Both the simulation quality and a low computational effort are needed to enable a controller optimization regarding different input signals. Models with lumped parameters are appropriated for this task. However, models with lumped parameters are not suitable for optimizing the exact geometric design. Due to the model simplifications, the number of physical interpretable parameters is low and many physical relationships between different parameters are omitted. For the coupling of different models and numerical solvers several approaches exist. In /5/ an overview about the state-of-art is presented. Probably, the best-known approach is the so-called co-simulation. Either different simulation tools run in parallel and exchange their results at certain times or a superordinate simulation calls a subordinate simulation to perform some calculations at certain times and to transfer the results. The simulation with lumped parameters including the control concept mostly represents the superordinate simulation stage. More detailed models of the subsystems are on the basis of FEM or CFD. For instance, in /6/, /7/ and /8/ detailed multibody simulations are subordinated to a simulation with lumped parameters to realize the closed-loop performance of machines and manipulators. In /9/ a subordinated transient FEM is performed for electrical machines and converters. The motivations of these contributions also focus on the simulation-based analysis and design. However, whenever design parameters are modified, a new controller design has to be performed. If this is not the case, the robustness of the controller and not the improvement of the system performance is evaluated. A complex controller design as in /4/ based on a co-simulation takes too much time and is not sustainable.

Another approach of combining different simulation methods is the parameterization of models with lumped parameters using simulation results of complex and detailed simulations like FEM. Regarding the simulation of electromagnetic actuators, the application of reluctance networks is well documented in the literature. This network method can transform the magnetic flux distribution within an actuator into an equivalent circuit with magnetic resistors. The structures of these reluctance models and the parameterization depend on the current flux distribution and the flux paths. Some examples are presented in /10/, /11/ and /12/ and show a high simulation quality. However, the chosen structure and the parameterization is not fully generalizable to different geometric designs and requires some human expertise whenever the geometrical design changes. The need of human interventions is not applicable in a fully automated optimization process. Another approach is to use static characteristic curves of the different subsystems within a model with lumped parameters. /13/ and /14/ utilize this approach for the simulation of a holistic system performance of a pressure relief valve and an electro-hydraulic actuator. The static simulations of FEM models of the electromagnetic actuators and CFD models of the hydraulic subsystem provide the static relationship between different quantities like current $i(t)$, force $F(t)$, pressure $p(t)$ and flow rate $Q(t)$. Nevertheless, models, limited to static characteristic curves, are only applicable for the closed-loop simulation if the impact of dynamic interactions like eddy currents can be neglected. The introduced papers, using the approach

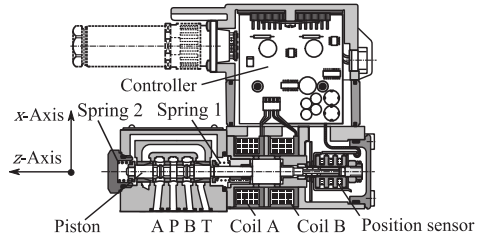


Figure 1: Cross-section of the proportional directional control valve 4WRREH6 /15/.

of the parameterization of lumped parameters by complex simulations, already show the possibility of the holistic model-based system optimization for selected systems. The contribution of this paper is a new holistic system parameterization and optimization process of a fast-acting proportional valve. This new approach relies on the model with lumped parameters in /16/ and /17/ and section 2.1, which is used for the evaluation of the closed-loop performance. This modeling approach enables a high simulation quality for valves with fast dynamics through the application of characteristic curves combined with linear dynamics. It has been proven in /18/ that this model is suitable for a model-based controller design for a proportional directional control valve. This model with lumped parameters is not only parameterized with the help of characteristic curves resulting from static FEM simulations. Whenever the design changes, the linear dynamics are identified using signals generated by a transient FEM simulation. This new system parameterization process aims to realize a fully automated system optimization to exploit the hidden potential of the current valve design. Optimization of the hydraulic subsystem is not a part of this new approach since hydraulic interactions are not considered during the controller design.

The next section presents the selected proportional valve and the closed-loop system. The valve model and the controller are parameterized by the process in section 3. The section 4 shows the closed-loop performance which is used for the evaluation of the current valve parameter setup. Finally, section 5 summarizes the results and provides an outlook on further work.

2 Closed-Loop System

The results of this contribution refer to the hydraulic proportional directional control valve 4WRREH6 of the company Bosch Rexroth AG /15/. Figure 1 presents the cross-section of the 4WRREH. A proportional directional control valve is used to route an oil flow from the pressure port P to the working ports A or B. The supply pressure $p(t)$ and the spool stroke $x_1(t)$ adjust the flow rate $Q(t)$ through the valve. While a working port is opened a pressure relief takes place on the other side between the tank T and the further working port. The control task is the fast and precise positioning of the stroke $x_1(t)$. An internal inductive sensor provides the current stroke. A sensor signal of $x_1(t) = \pm 100\%$ indicates a fully opened working port A or B. To achieve high dynamics the electromagnetic actuator has a double stroke solenoid. The two coils operate in contrary motion directions. Movement is mainly characterized by the actuator and not by pre-loaded springs. Nevertheless, two preloaded springs contribute certain forces. These nearly equal pre-loaded springs ensure the force-type connection of the movable parts. To simulate the valve closed-loop performance a suitable holistic model is required. The holistic performance of this valve is evaluated using the closed-loop performance of the stroke respectively position control regarding different criteria like rise time, settling time and overshoot characteristics.

2.1 Valve Model with Lumped Parameters

In the previous work in /16/, /17/ and /18/ an electromagnetic actuator with a single coil which acts against a pre-loaded spring is investigated. The developed model is now ported and extended to the double stroke valve. Figure 2 illustrates the overall system model. It is divided into two current models, a force model and a mechanics model. The actuator input voltages are mapped to the electrical currents which are used to simulate the actuator force. This force leads to a movement of the spool. The linear dynamics $G_A(s)$, $G_B(s)$, and $G_F(s)$, exhibit purely

mathematical parameters. These parameters have no physical interpretation. However, the analysis of the force model shows clearly the necessity of these dynamics. A sudden change in a current signal $i_A(t)$ or $i_B(t)$ at the input of the force curves $F_s(i_A, i_B, x_1)$ leads to a sudden change of the static force $F_{stat}(t)$. In reality, dynamic effects occur within the actuator as eddy currents. A magnetic flux linkage $\psi(t)$ and thus also the force $F(t)$ only reach the value pre-determined by the static characteristics after a certain delay. The linear force dynamics model this effect. It is a kind of dynamic correction of the static model approach. From a system-theoretical point of view, the combination of a static nonlinearity with linear dynamics is a common model approach and is called Hammerstein Model. Since the relationship between the current $i(t)$ and the flux linkage $\psi(t)$ is used in an inverted manner within the current models, the current dynamics exhibit a more derivative character. The amplitudes of the currents $i_{stat,A}(t)$ and $i_{stat,B}(t)$ at the outputs of the static curves $i_{s,A}(\psi_{stat,A}, i_B, x_1)$ and $i_{s,B}(\psi_{stat,B}, i_A, x_1)$ within the current models are too low. The linear dynamics increase the current amplitudes. Since a double stroke solenoid is used, two separated models are utilized. The basic approximation for every current model is the differential equation like it is described in /19/:

$$V_{PWM}(t) = V_R(t) + V_L(t) = i(t) R + \frac{d\psi(x_1(t), i(t))}{dt} \quad (1)$$

This assumption is only valid for slow-acting actuators when dynamical effects like eddy currents can be neglected. The actuator input signals $V_{PWM,A}(t)$ and $V_{PWM,B}(t)$ are pulse-width modulated voltage signals. Since the coils are built identically, the assumption of identical behavior is valid. It applies $G_A(s) = G_B(s)$ and equal ohmic coil resistors $R_A = R_B$. FEM simulations show magnetic field coupling of the separated coils. Thus, the characteristic curves do not only depend on their own current $i_A(t)$ or $i_B(t)$ and the stroke $x_1(t)$. The further dependency on the current in the other coil is modeled as a simple cross coupling. The one dimensional movement of the movable parts as armature and spool constitutes a second order differential equation (mass-spring-damper) with a nonlinear friction term:

$$F_f(v(t)) = F_h \frac{1}{1+e^{-\alpha v(t)}} - \frac{F_h}{2} + \beta v(t) \quad (2)$$

with the static friction F_h , an approximation parameter α and the damping coefficient β . The variable $v(t) = \dot{x}_1(t)$ is the spool velocity. The spring constants c_1 and c_2 represent the two springs. A fast change of the armature position (step-shaped) also leads to dynamic effects within the actuator. These effects are neglected in this model since the impact is significantly lower compared to the impact of fast changing electrical signals. Usually, fast position changes only occur when hydraulic loads are applied. Hydraulic loads are not investigated in this work since the valve's controller parameters are optimized with mechanically closed working ports A and B. Further, more detailed information, concerning the model with lumped parameters is presented in /16/, /17/ and /18/.

2.2 Cascaded Control Concept

The structure of the cascaded valve native control concept is adopted. The inner simple current controllers are maintained. Figure 2 presents the native control structure. However, the complex outer position controller is replaced with a model predictive concept as it is described in /20/. Since the plant is known exactly during offline simulations, it can be used as a part of an advanced control concept. In this way, the number of classic controller parameters can be reduced significantly. In /20/ it has been proven that the sub-optimal model predictive trajectory set control (MPTSC) is real-time capable for the valve's native sampling frequency of $f_s = 10$ kHz with a closed-loop performance similar to the nonlinear PID controller. The native current controller including the function of the power electronics become a part of the valve model. In every control sampling interval of the native controller of $t_s = 1/10$ kHz the voltage level can be inverted once by a hardware processing unit. The sampling frequency of this unit is above $f_s > 1$ GHz. For reasons of simplification, during the simulation of the valve model the native controller sampling interval is divided into eight equal time steps resulting in a simulation step size of $t_s = 1/80$ kHz for the plant. For the remaining sections, the controller design only focuses on the position controller. A state space controller as the MPTSC requires all j states $\mathbf{x}(t) = [x_1(t), x_2(t), \dots, x_j(t)]^T$ of the plant. The native nonlinear PID controller only requires the stroke $x_1(t)$.

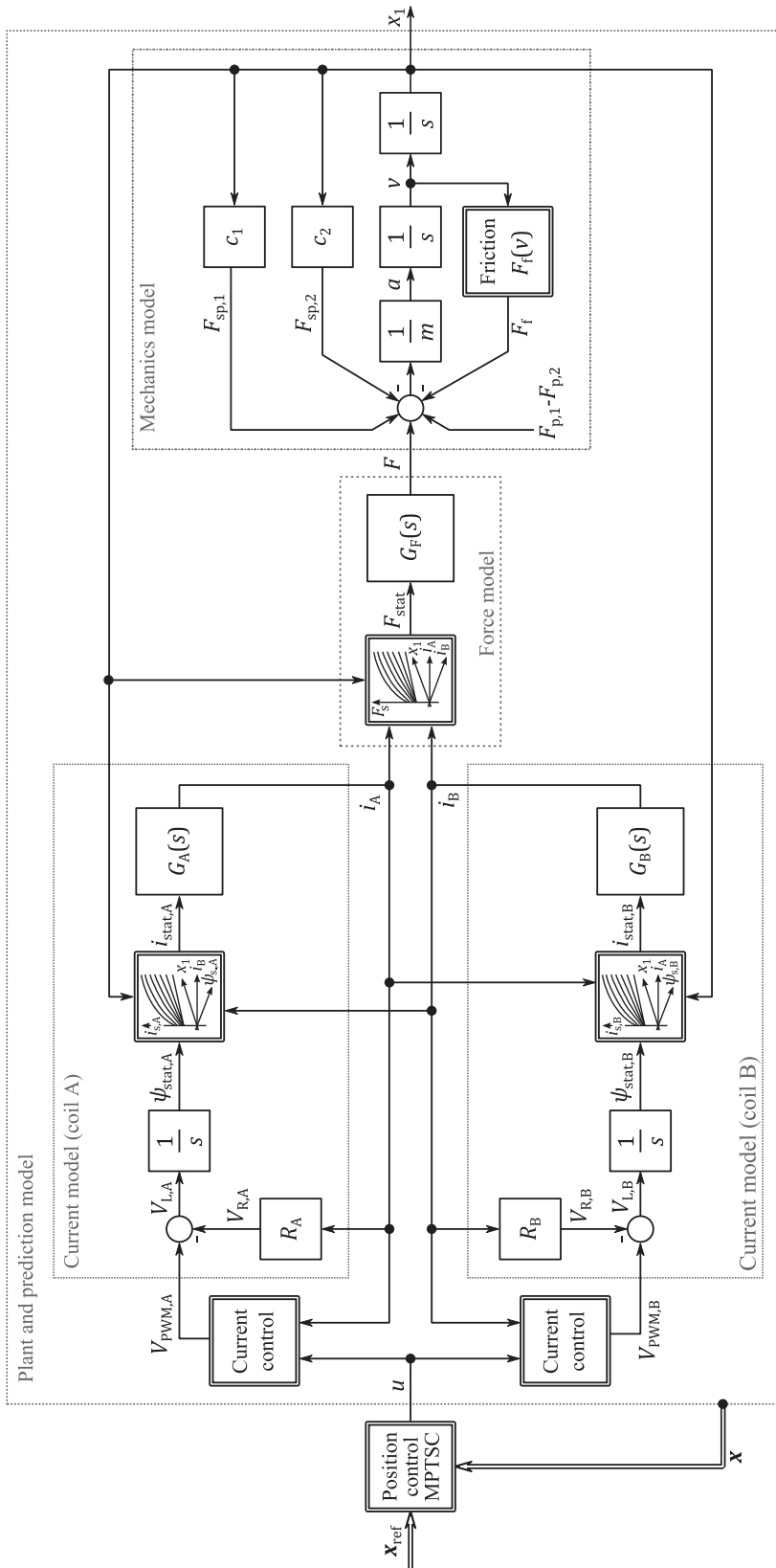


Figure 2: Overall valve model with lumped parameters which is used to evaluate the holistic system performance regarding the closed-loop.

3 Parameterization Process of the Valve Model

The closed-loop system in section 2 is well suited to evaluate the valve performance or to be used in a model-based controller design. However, the physical relationship between the parameters is insufficient due to the model simplifications. For instance, when changing the coil windings the ohmic resistance and the magnetic characteristics change. In the model in section 2.1 there is no relationship between the characteristic curves and the ohmic resistors R_A and R_B . When optimizing directly the parameters within the model with lumped parameters, the characteristic curves must be described by means of polynomial functions. The coefficients of the applied polynomial functions must then depend on the current $i(t)$ and the stroke $x_1(t)$. The additional resulting parameters can be subjected to an optimization. It would be determined how a characteristic curve should look like to provide an improvement in the closed-loop performance. However, the impact of a change of the shape of the characteristic curves on the ohmic resistor, on the movable mass or on the linear dynamics is not reproduced by the model. Furthermore, it is difficult to determine the parameter ranges of this additional polynomial coefficients. Characteristic curves which can be realized technically are not known in advance. Moreover, the mapping of characteristic curves to geometrical design parameters depends on human expertise. Due to its nonlinearity and its fast dynamics, the actuator represents the most significant challenge for the closed-loop control. The idea is to increase the level of detail of the electromagnetic actuator by including a FEM model. Within this model, the coupling of the parameters is more accurate in comparison to a model with lumped parameters. For the FEM simulation a 2D actuator model of the 4WRREH6 is solved applying Ansys Maxwell. For simplification, a rotational symmetry around the z -axis (armature movement direction) is assumed. Figure 1 shows the axes of the 2D FEM model. A new parameterization process of the valve model in section 2.1 based on FEM data is presented in Figure 3. Model parameters which depend on the geometrical design are adjusted as soon as the design of the actuator changes.

3.1 Conversion of Geometrical Design Parameters to Physical Model Parameters

The valve model with lumped parameters is parameterized by geometrical design data and physical parameters. Firstly, some geometrical design changes of the actuator lead to new resistor and mass values. If the spool dimensions or the coil turns are changed, the resistor values R_A and R_B change too. The orthocyclic winding of the coil describes a relationship between the 2D spool dimensions $l_x \times l_z$, the number of coil turns λ and the wire gauge including the isolation d_w :

$$h(l_x, \lambda, d_w) = [1 + (\zeta(l_x, \lambda) - 1) \sin(60^\circ)] d_w \quad (3)$$

The parameter $\zeta(\cdot)$ is the number of wire layers and $h(\cdot)$ the winding height in the x -direction. The wire gauge is chosen considering the DIN standard EN IEC 60317-0-1 which specifies the characteristics of copper winding wires. Using the specific resistance and the radius between the axis of rotation (z -axis) and each coil winding center the resistor values R_A and R_B can be calculated. When the armatures dimensions change during the optimization the mass of the armature, and thus the overall movable mass m , is also adjusted. Therefore, the 2D armature dimensions and the armature material mass density are utilized. The level of detail is not increased for the mechanical subsystem compared to /6/, /7/ or /8/. Hence, there are further parameters which can be provided directly to the valve model. These include the spring constants c_1 and c_2 and the spring pre-load forces $F_{p,1}$ and $F_{p,2}$. The friction parameters of the function $F_f(v(t))$ are kept constant concerning the reference design since an adjustment is not possible with this low level of detail within the mechanics model.

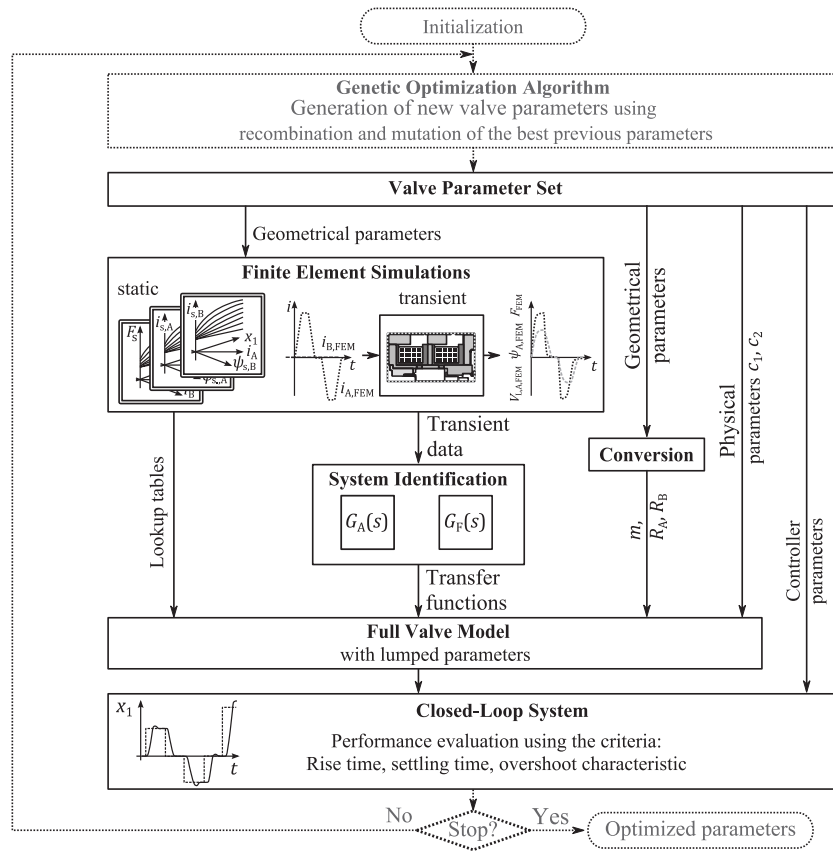


Figure 3: Holistic approach to the system optimization of a fast-acting proportional valve. Dynamic effects are identified based on FEM data.

3.2 Identification of Valve Dynamics

A change in the actuator's geometrical design has an impact on the static behavior as well on the dynamic interactions within the electromagnetic subsystem. The identification procedure of dynamics requires input and output signals. In [16], [17] and [18] measurable signals are investigated. The unmeasurable force during real operation of the valve is reconstructed by the measurable position signal and with the help of the inverse mechanics model. In contrast, within this work, signals simulated by the transient FEM are used for the identification process. Figure 4 presents an overview about the whole identification procedure. An electrical network is not modeled within the FEM. Thus, the electrical current constitutes the excitation signal within the transient FEM simulation. The induced voltage $V_{L,A,FEM}(t)$, the dynamic flux linkage $\psi_{A,FEM}(t)$ and the dynamic force $F_{FEM}(t)$ represent the required and simulated FEM quantities. Regarding the model with lumped parameters, the current is the connecting signal between the current and force model. To identify the linear dynamic $G_A(s)$ the input signal $i_{stat,A}(t)$ and the output signal $i_{A,FEM}(t)$ are needed. The variable $i_{A,FEM}(t)$ is the excitation signal and $i_{stat,A}(t)$ is unknown at first. It is the case that the input signal as well as the dynamics parameter are unknown. The left plot of Figure 5 shows the induced voltage $V_{L,A,FEM}(t)$ in coil A as a result of the transient FEM using a pre-defined excitation signal. The left plot of Figure 6 shows the associated excitation signal (trapezoidal shape). The variable T represents a time constant. Figure 4.a) summarizes this first needed action to generate identification data. The current in coil B is kept constant at $i_{B,FEM}(t) = 1A$ and the position is kept constant at $x_{1,FEM}(t) = 0\%$. The

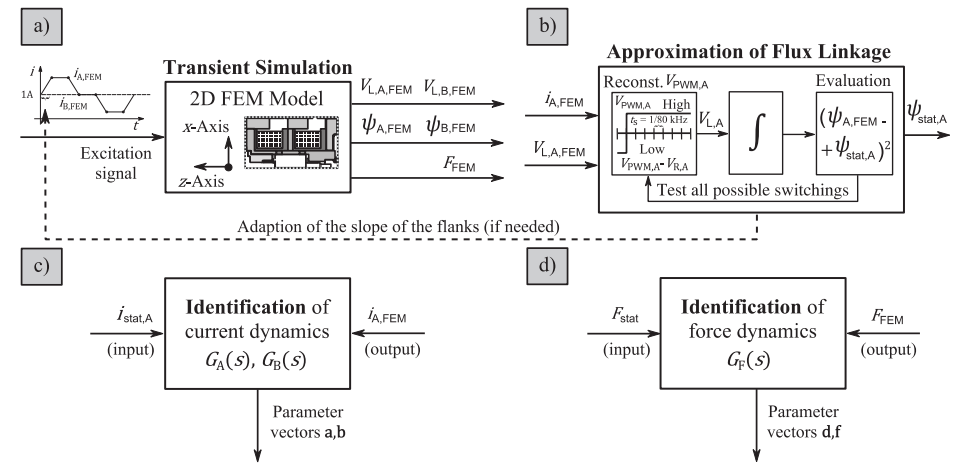


Figure 4: General overview about the necessary steps during the identification process of the linear dynamics. a): The linear dynamics within the valve model are identified based on transient FEM results. b): The reconstruction of the pulse-width modulated input voltage $V_{PWM,A}(t)$ is required to estimate an input signal $i_{stat,A}(t)$. It should be proofed if this signal could also be simulated with the valve model. c) and d): The utilized input and output signals for the identification of the linear dynamics are shown.

smooth magnetic flux linkage generated by the FEM cannot be reproduced by the model approach in section 2.1 since the input of the current model is a pulse-width modulated voltage signal. Hence, it makes no sense to use the FEM flux linkage signal $\psi_{A,FEM}(t)$ at the input of the characteristic curve $i_{s,A}(\psi_{stat,A}, i_B, x_1)$ to calculate the dynamics input signal $i_{stat,A}(t)$. With the knowledge of the shape of pulse-width modulated actuator input voltage $V_{PWM,A}(t)$ and the function of the power electronics described in section 2.2, the smooth flux linkage signal can be approximated $\psi_{A,FEM}(t)$ with $\psi_{stat,A}(t)$. Figure 4.b) illustrates the approximation action. For the approximation of the FEM induced voltage $V_{L,A,FEM}(t)$ by equation (1), which is also simulated with a fixed step size of $t_s = 1/10$ kHz, the pulse-width input signal $V_{PWM,A}(t)$ is reconstructed. For every simulated FEM vector element, all 16 possible combinations of the input voltage signal are tested. As already mentioned, the model with lumped parameters including the power electronics is simulated with $f_s = 80$ kHz. Within a sampling interval of $t_s = 1/10$ kHz of the outer controller, there are 16 possibilities of inverting the voltage level during a sampling interval step. One of 16 possible switching actions is illustrated in Figure 4.b). If the first voltage value at the beginning of a sampling interval is fixed, then only eight possibilities exist. The switching sequence which leads to the minimal quadratic error between the flux linkage signal $\psi_{A,FEM}(t)$ simulated by transient FEM and the approximated flux linkage signal $\psi_{stat,A}(t)$ by equation (1), regarding the current sampling interval, is chosen. Figure 5 illustrates the resulting approximation of the induced voltage $V_{L,A,FEM}(t)$ (based on the reconstructed input voltage $V_{PWM,A}(t)$) and the magnetic flux linkage $\psi_{A,FEM}(t)$. The time integration of the induced voltage leads to the magnetic flux linkage in the right plot of Figure 5. The comparison with the results of the transient FEM, highlights the high but limited quality of approximation. Only high amplitudes of induced voltages cannot be reproduced by the valve model with lumped parameters. This results in an increasing approximation error (for example at $t = 4.8T$). A fast current change leads to a high amplitude of the induced voltage. Hence, a suitable current excitation signal is required for generating identification signals. For instance, a step-shaped excitation signal would lead to high amplitudes of the induced voltage. Thus, the trapezoidal shaped excitation signal with a variable steepness of the flanks constitutes a possible approach. For this reason, Figure 4.b) shows a feedback to Figure 4.a). If a geometric design leads to highly dynamic electromagnetic interactions within the actuator, the slope of the flanks can be reduced automatically. The fit of the approximation of the FEM flux signal $\psi_{A,FEM}(t)$ indicates a poorly conditioned excitation signal. Regarding the force model, no requirements exist for the current excitation signal

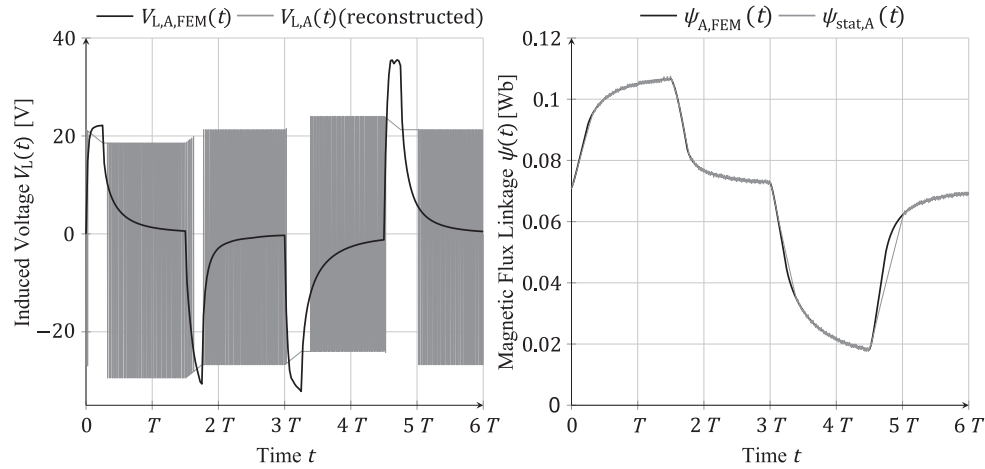


Figure 5: Approximation of the transient FEM signals with pulse-width modulated voltage inputs. Left: Approximation of the induced voltage $V_{L,A,FEM}(t)$ with the reconstructed input $V_{PWM,A}(t)$. The model with lumped parameters cannot represent sufficiently high voltage values. The current excitation signal must be chosen in consideration of this effect. Right: Time integration of the left voltage signals leads to the magnetic flux linkage.

since the input $F_{stat,A}(t)$ and the output $F_{FEM}(t)$ are well known. However, the trapezoidal signal is also used for the identification of $G_F(s)$. The current excitation signal is designed to be relatively short while magnetizing in both directions starting from $i_{A,FEM}(t) = i_{B,FEM}(t) = 1A$. The stroke is kept constant with $x_1(t) = 0\%$. The short time base is chosen since linear dynamics with just a small number of parameters **a**, **b**, **d** and **f** are utilized:

$$G_A(s) = G_B(s) = \frac{b_0 + b_1s + b_2s^2}{1 + a_1s + a_2s^2}, \quad G_F(s) = \frac{f_0 + f_1s + f_2s^2}{1 + d_1s + d_2s^2} \quad (4)$$

Figure 4.c) and Figure 4.d) show the identification actions of the dynamics based on transient FEM results. In the case of a more complex excitation signal with different levels of excitation, the linear models would try to fit on average to the simulated transient FEM results. When modeling a nonlinear system with a linear model structure the parameters depend on the excitation signal. This problem is well known from the literature and is discussed and summarized in [21]. Figure 6 shows the identification performance for the current dynamics on the left side and for the force dynamics on the right side. The objective is to realize suitable correction properties of the dynamics. The dynamics do not aim to realize an exact match. The results on the left side show the desired derivative characteristics of the current dynamics and the results on the right side show the desired delayed force application. Hence, the desired correction properties of the dynamics can be achieved with this approach. The use of simple dynamics with a small number of parameters justifies a neglect of a test procedure to avoid overfitting. This fact reduces computational time of the FEM. Obviously, it is possible to use non-linear dynamic models for the improvement of the valve model instead of linear dynamics. For this purpose, a division of the simulated FEM results at least into a training and test set would be necessary. The simple shape of the chosen excitation provides a further advantage concerning computational effort. The fixed step size of the transient FEM can be chosen higher as the step size during the closed-loop control. Since an identification is performed for a model of the continuous time domain, the dependency on the sampling step size is rather low. This, however, requires the use of a solver for nonlinear optimization problems. For the identification of linear dynamics in the time domain representation, a nonlinear least-squares problem is usually solved with a Newton-type solver.

4 Development of the Holistic Valve System Optimization Process

To evaluate the impact of the design variations on the system performance, a controller design process is essential. It makes sense to include the controller parameters into the set of optimization parameters. However, the problem

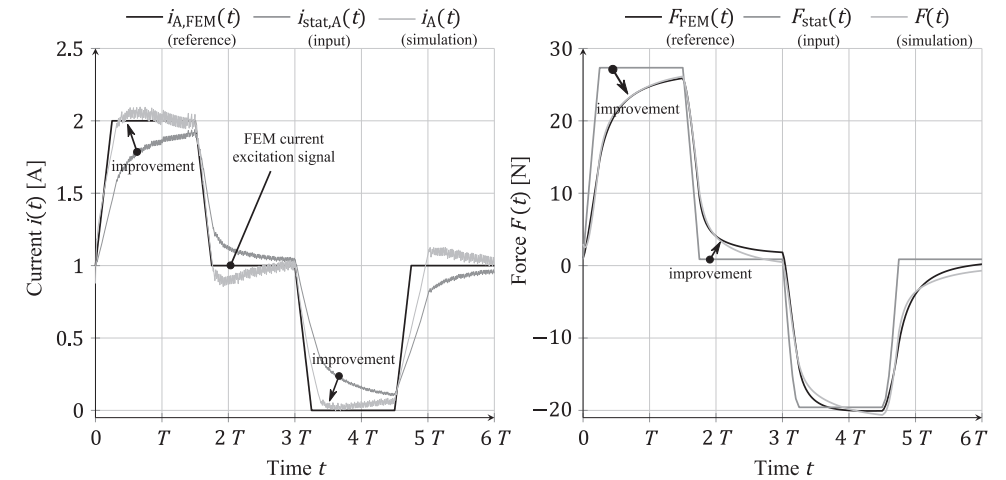


Figure 6: Identification results of the linear dynamics $G_A(s)$ and $G_F(s)$. The dynamics adjust the signals at the outputs of the characteristic curves towards the transient FEM signals. Left: Derivative character of the current dynamics. Right: Delayed force application through the usage of the force dynamics.

is the high number of controller parameters regarding the native nonlinear PID position controller. The global optimization algorithm may not achieve convergence within an acceptable time. To reduce the number of controller parameters significantly, a model predictive control concept is suitable. In this case, the whole plant is a part of the control concept and is known exactly during the optimization through the parameterization process in Figure 3. Figure 7 illustrates the closed-loop performance of the proportional valve with the reference design. The model with lumped parameters is parameterized applying the process in Figure 3 and the valve reference design. MPTSC with only three parameters is tuned to reach a closed-loop performance which is similar to the native nonlinear PID control concept. This three additional parameters can be included into an optimization vector. Thus, the assumption is that the extension of the system optimization vector with three controller parameters has only a low impact on the global optimization process. The current signals $i_A(t)$ and $i_B(t)$, the input signal $u(t)$ and the stroke signal $x_1(t)$ exhibit valve common characteristics. The closed-loop performance regarding the position can be now used to evaluate different criteria as rise times, settling times and overshoots concerning different reference step amplitudes for the varying design. Whenever the design changes the prediction model is adopted inherently. The current signals can be used to define additional constraints like maximum power losses. A suitable optimization algorithm for multi-criteria optimization problems like the NSGA-II [22] modifies the values of a pre-defined optimization vector. Elements of this optimization vector can either be geometrical, physical or controller parameters. In Figure 3 the optimization algorithm constitutes the outer loop. Although the model predictive approach reduces the number of controller parameters, there are still plenty of different geometrical parameters. To realize a useful system optimization, a pre-selection of the essential parameters is required. A sensitivity analysis contributes the needed information. Every construction parameter is changed by a factor of $\pm 5\%$ while the other parameters are kept constant. A static and a transient FEM simulation provide the sensitivity. The maximum changes in the characteristic curves and the pole-zero description of the linear dynamics are considered. Since the FEM is time-consuming, a global sensitivity analysis is not performed. An important consideration for the sensitivity analysis or the optimization is the adherence to restrictions concerning not recommended design. For instance, adherence to certain dimensions provided by human expertise, avoiding additional air gaps or overlap of different FEM elements should be taken into account. For this reason, the distantly a FEM element is related to an axis (x -axis or z -axis) the more dependencies it exhibits from more nearby related elements and thus geometrical parameters. Thus, the dimensions of the outer elements depend on the dimensions of the elements near the axes. The optimization process and the valve model are simulated with Matlab/Simulink.

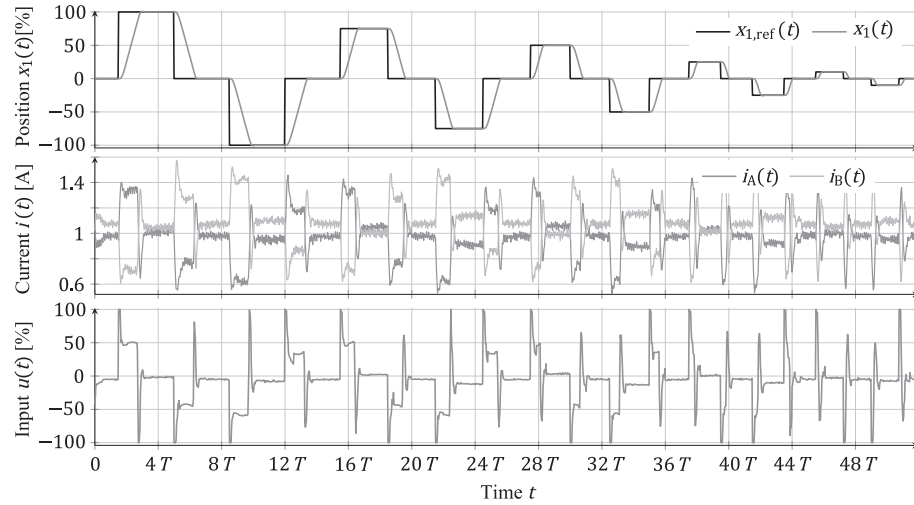


Figure 7: Evaluation of the model-based valve system performance. The valve model is identified with FEM data which is generated with the original valve design. Top: Closed-loop performance regarding the position control. The overall objectives are the rise times, the settling times and the overshoot characteristics. Middle: Current signals of the two coils during closed-loop control. Bottom: Constrained input signal with $|u(t)| \leq 100\%$.

The closed-loop system, including the plant and the prediction model, is simulated with a fixed step size and finite-differences using the Euler method:

$$\mathbf{x}_{k+1} = \mathbf{x}_k + \mathbf{f}(\mathbf{x}_k, u_k) t_s, \mathbf{x}_{k=0} = \mathbf{x}_0. \quad (5)$$

The vector $\mathbf{x}_k \in \mathbb{R}^j$ describes the state vector with j states at time instance k and $u_k \in \mathbb{R}$ the corresponding input. $\mathbf{f}(\cdot)$ denotes the nonlinear system dynamics concerning the whole model in Figure 2. The inter-process communication between Matlab and Ansys is fully automated utilizing the OLE Automation and the scripting functions of Ansys Maxwell. However, this contribution does not aim to discuss the optimization process and the FEM model in detail. The primary objective is to introduce the identification of dynamics within a fully automated optimization process. The overall parametrization process enables a holistic system optimization of a proportional directional control valve.

5 Summary and Conclusion

This contribution presents a novel holistic approach to the system optimization process of a fast-acting proportional valve. A model with lumped parameters enables the simulation of the closed-loop performance and thus the evaluation of the holistic system performance. By utilizing a 2D FEM model of the electromagnetic actuator within the optimization loop, the level of detail of this nonlinear subsystem increases. A process is developed which maps geometrical design parameters to the required model parameters. For the simulation of dynamical effects like eddy currents of fast-acting electromagnetic actuators linear dynamics are identified based on transient FEM simulation results. The parameterization with FEM data results in a closed-loop system which shows a realistic closed-loop performance. This new parameterization process is fully automated and is suitable for the holistic valve system optimization without requiring human expertise. Further work is concerned with the description of the optimization setup in more detail. The progress of the evolution and the discussion of the results are of central interest.

Nomenclature

Variable	Description	Unit
$\mathbf{a}, \mathbf{b}, \mathbf{d}, \mathbf{f}$	Parameter vectors of linear dynamics	[-]
c_1, c_2	Spring constants	[N/m]
d_w	Diameter of wire with isolation	[m]
$e(t)$	Position error	[%]
$\mathbf{f}(\cdot)$	Nonlinear system dynamics	[-]
$F(t)$	Actuator force	[N]
$F_f(v(t))$	Velocity dependent friction	[N]
$F_{FEM}(t)$	Actuator force from transient FEM	[N]
F_h	Static Friction	[N]
$F_{p,1}, F_{p,2}$	Spring pre-load forces	[N]
f_s	Sampling frequency	[Hz]
$F_s(\cdot)$	Characteristic force curves from transient FEM	[N]
$F_{sp,1}, F_{sp,2}$	Spring forces	[N]
$F_{stat}(t)$	Output of characteristic curves within the force model	[N]
$G_A(s), G_B(s)$	Transfer function of current dynamics for coil A and B	[-]
$G_F(s)$	Transfer function of force dynamics	[-]
$h(\cdot)$	Winding height of orthocyclic coil winding	[m]
$i(t)$	Electrical current	[A]
$i_A(t), i_B(t)$	Electrical current for coil A and B	[A]
$i_{A,FEM}(t), i_{B,FEM}(t)$	Current excitation for transient FEM for coil A and B	[A]
$i_{s,A}(\cdot), i_{s,B}(\cdot)$	Characteristic current curves for coil A and B from static FEM	[A]
$i_{stat,A}(t), i_{stat,B}(t)$	Output of characteristic curves within current models A and B	[A]
j	Number of states of valve model	[-]
l_x, l_z	Coil cross-section dimensions within FEM	[m]
m	Mass of all movable elements	[kg]
$p(t)$	Oil pressure	[bar]
$Q(t)$	Volumetric flow rate	[m ³ /s]
R_A, R_B	Ohmic resistor for coil A and B	[Ω]
T	Time constant	[s]
t_s	Sampling interval	[s]
$u(t), u_k$	Output of position controller, u at time instance k	[%]
$v(t)$	Velocity	[%/s]

$V_L(t)$	Induced voltage	[V]
$V_{L,A}(t), V_{L,B}(t)$	Approximation of induced voltage for coil A and B	[V]
$V_{L,A,FEM}(t), V_{L,B,FEM}(t)$	Induced voltage for coil A and coil B from transient FEM	[V]
$V_{PWM}(t)$	Pulse-width modulated voltage	[V]
$V_{PWM,A}(t), V_{PWM,B}(t)$	Pulse-width modulated input voltage for coil A and B	[V]
$V_R(t)$	Ohmic voltage drop	[V]
$V_{R,A}(t), V_{R,B}(t)$	Ohmic voltage drop for coil A and coil B	[V]
$\mathbf{x}(t), \mathbf{x}_k$	State vector of the plant, \mathbf{x} at time instance k	[-]
$\mathbf{x}_{ref}(t)$	Reference state vector for control	[-]
$x_1(t)$	Stroke, position	[%]
$x_{1,ref}(t)$	Reference position for control	[%]
$\psi(t)$	Magnetic flux linkage	[Wb]
$\psi_{stat,A}(t), \psi_{stat,B}(t)$	Approximation of flux linkage for coil A and B	[Wb]
$\psi_{A,FEM}(t), \psi_{B,FEM}(t)$	Flux linkage for coil A and B from transient FEM	[Wb]
α, β	Friction model parameters	[-], [Ns/m]
λ	Number of coil turns	[-]
$\zeta(\cdot)$	Number of winding layers in x -axis direction	[-]

References

/1/ Thramboulidis, K., *Challenges in the development of Mechatronic systems: The Mechatronic Component*, In: IEEE International Conference on Emerging Technologies and Factory Automation, Hamburg, pp. 624-631, 2008.

/2/ Amerongen, J., *Mechatronic design*, In: Mechatronics, Vol. 13, No. 10, pp. 1045-1066, 2003.

/3/ Åström, K., and Hägglund, T., *The future of PID control*, In: Control Engineering Practice, Vol. 9, No 11, pp. 1163-1175, 2001.

/4/ Krettek, J., Schauten, D., Hoffmann, F., Bertram, T., *Evolutionary Hardware-in-the-Loop Optimization of a Controller for Cascaded Hydraulic Valves*, In: IEEE/ASME International Conference on Advanced Intelligent Mechatronics, AIM 2007, Zürich, Switzerland, pp. 1-6, September 2007.

/5/ Geimer, M., Krüger, T., Linsel, P., *Co-Simulation, gekoppelte Simulation oder Simulatorkopplung? Ein Versuch der Begriffsvereinheitlichung*, In: O+P Ölhydraulik und Pneumatik, Vol. 50, No, 11-12, pp. 572-576, 2006.

/6/ Reinhart, H., Weissenberger, M., *Multibody simulation of machine tools as mechatronic systems for optimization of motion dynamics in the design process*, IEEE/ASME International Conference on Advanced Intelligent Mechatronics (Cat. No.99TH8399), Atlanta, GA, USA, pp. 605-610, 1999.

/7/ Samin, J. C., Brüls, O., Collard, J. F., Sass, L., Fiset, P., *Multiphysics modeling and optimization of mechatronic multibody systems*, In: Multibody System Dynamics, Vol. 18, No. 3, pp 345-373, 2007.

/8/ Brezina, T., Hadas, Z., Vetiska, J., *Using of Co-simulation ADAMS-SIMULINK for development of mechatronic systems*, 14th International Conference Mechatronika, Trencianske Teplice, pp. 59-64, 2011.

/9/ Kanerva, S., Kaukonen, J., Szucs, A., Hautamaki, T., *Coupled FEM-Control Simulation in the Analysis of Electrical Machines and Converters*, In: 12th International Power Electronics and Motion Control Conference, pp. 1925-1930, Portoroz, 2006.

/10/ Fiedler, M., Helduser, S., *Model Based Optimisation of a Servo-Pneumatic Valve*, In: 6th International Fluid Power Conference, Workshop Proceedings, 6. IFK, Dresden, Germany, pp. 127-137, March 31, 2008.

/11/ Wehner, D., Helduser, S., Weber, J., Schoppel, G., *Reluctance Network for Simulation of Proportional Solenoids in Fluid Power Valve Systems*, In: Proceedings of Fluid Power and Motion Conference, pp. 129-144, 2010.

/12/ Fiedler, M., Helduser, S., Wehner, D., *Coupled Simulation for the Virtual Product Development of Electro-Hydraulic Valves*, In: 7th International Fluid Power Conference, 7. IFK, Aachen, Germany, March 22-24, 2010.

/13/ Erhard, M., Schoppel, G., Weber, J., *Simulation-Based Design of a Direct-Operated Proportional Pressure Relief Valve*, In: 8th International Fluid Power Conference, 8. IFK, Dresden, Germany, pp. 33-44, March 26-28, 2012.

/14/ Poltschak, F., Koch, O., Farrokhzad, B., Amrhein, W., Weber, J., *Multi Domain Mechatronic Optimization of an Intelligent Electro-Hydraulic Actuator*, In: 8th International Fluid Power Conference, 8. IFK, Dresden, Germany, March 26 - 28, 2012.

/15/ Bosch Rexroth AG, *Type 4WRREH 6; 4/3 directional control valve, directly controlled, with electrical position feedback and integrated electronics (OBE)*, Datasheet, Version RE 29041/03.10.

/16/ Makarow, A., Braun, J., Krimpmann, C., Bertram, T., Schoppel, G., Glowatzky, I., *Regelungstechnische Modellierung eines hydraulischen Wegeventils*, In: VDI/VDE Mechatroniktagung, Dortmund, Germany, pp. 203-208, March, 2015 (in German).

/17/ Makarow, A., Braun, J., Krimpmann, C., Bertram, T., Schoppel, G., Glowatzky, I., *System Model of a Directional Control Valve for Control Applications*, In: The Fourteenth Scandinavian International Conference on Fluid Power, Tampere, Finland, May, 2015.

/18/ Krimpmann, C., Makarow, A., Bertram, T., Glowatzky, I., Schoppel, G., Lausch, H., *Simulationsgestützte Optimierung von Gleitstandsreglern für hydraulische Wegeventile*, In: at-Automatisierungstechnik 2016, Vol. 64, No. 6, pp. 443-456, June, 2016 (in German).

/19/ Kallenbach, E., Eick, R., Quendt, P., Ströhla T., Feindt, K., Kallenbach M., Radler, O., *Elektromagnete: Grundlagen, Berechnung, Entwurf und Anwendung*, 4., überarbeitete und erweiterte Auflage, Vieweg+Teubner Verlag, Wiesbaden, Germany, 2012 (in German).

/20/ Makarow, A., Keller, M., Rösmann, C., Bertram, T., Schoppel, G., Glowatzky, I., *Model Predictive Trajectory Set Control for a Proportional Directional Control Valve*, In: IEEE Conference on Control Technology and Applications (CCTA), Kohala Coast, Hawai'i, August, 2017.

/21/ Schoukens, J., Vaes, M., Pintelon, R., *Linear System Identification in a Nonlinear Setting: Nonparametric Analysis of the Nonlinear Distortions and Their Impact on the Best Linear Approximation*, In: IEEE Control Systems, Vol. 36, No. 3, pp. 38-69, June, 2016.

/22/ Deb, K., Pratap, A., Agarwal, S., Meyarivan, T., *A fast and elitist multiobjective genetic algorithm: NSGAII*, In: IEEE Transactions on Evolutionary Computation Vol. 6, pp. 182-197, 2002.